Jurnal Teknologi

Full Paper

EFFECT OF LATERAL AND AXIAL ECCENTRIC LOADS OF NAILED-SLAB SYSTEM

Kusrin[a]*, Pratikso[a], Abdul Rochim[b]

[a]Doctoral Program in Civil Engineering, Faculty of Engineering, Sultan Agung Islamic University, 50112, Semarang, Central Java, Indonesia
[b]Faculty of Engineering, Sultan Agung Islamic University, 50112, Semarang, Central Java, Indonesia

Article history
Received
21 April 2025
Received in revised form
23 July 2025
Accepted
4 August 2025
Published Online
30 April 2026

*Corresponding author
kusrin@usm.ac.id

Graphical abstract

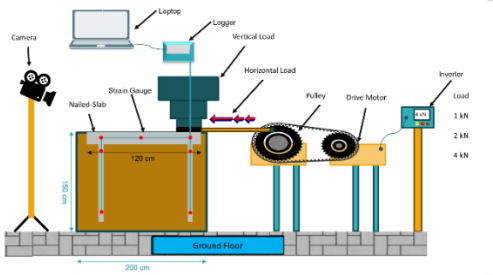

Abstract

Rigid pavement with Nailed-slab system is a development of the chicken claw method that changes the pavement shell of the chicken claw system with short piles. One of the most important things in designing rigid pavements with a Nailed-slab system is lateral and eccentric loads. This study aims to determine the influence of lateral and axial loads on the behavior of pavement slabs, including the influence of gaps due to lateral loads on the bearing capacity of pillars and the deflection of pavement slabs on Demak soft soils. The results showed that Demak soft soil had a shear strength of 21.4 kPa with a moisture content of 33.1% with a fine grain dominance of 93.2%. The rigid-slab system exhibits significant initial deflection and shift due to the presence of eccentric and lateral axial loads, but still achieves stability within safe limits for applications in Demak soft soils. The gaps that occur due to lateral loads cause significant pile shifts at the beginning of the phase, reducing temporary bearing capacity and increasing slab deflection. However, the pavement structure remains stable after reaching a gradual shift pattern.

Keywords: Rigid pavement, soft soil, nailed-slab system, eccentric loads, lateral axial loads

1.0 INTRODUCTION

Road pavement is important to ensure safety, driving comfort and durability of road structures. Damage to the pavement is difficult to identify clearly, but it will gradually worsen with an increase in traffic load [1]. Damage to road pavements is surface imperfections related to damage to vehicles and the environment, long material life, and poor construction structures [2]. Highway performance in the long term is influenced by vehicle loads and environmental factors such as temperature variations. Conventional road pavements and pedestrian paths in urban areas usually use rigid to semi-rigid waterproof structures [3]. The ambient air temperature controls the heat convection at the ground level and plays an important role in the temperature distribution on the slabs which is simultaneously affected by other weather conditions such as wind speed and solar radiation [4]. Fluctuating temperatures can cause road damage, including uneven deformation and thermal cracks in pavements. In contrast to road

structures, natural soil saturation is usually high due to groundwater infiltration and rainfall [5].

Soft soil is a type of fine-grained soil with high moisture content, saturation degree, porosity, porosity, initial pore water pressure so that it has low shear strength with large compressive power in the event of an increase in effective stress. Soft soil is one of the obstacles in road construction because the carrying capacity of soft soil is very low, which can cause unstable road pavement on soft soil [6]. Rigid pavement is generally used on soft subsoils. Rigid pavement consists of an elastic concrete slab or joint slab resting on a supporting foundation modeled as a spring and dashpot system or a homogeneous or layered half-chamber [7]. The pavement is located in a pile on soft soil so that the subsidence that occurs tends to be differential settlement in the transverse direction or lengthening the road trajectory as a result of uneven load distribution along the width or length of the pavement or due to soil inhomogeneity. The pavement will receive a load as a result of the temperature which causes the pavement to experience a bending moment back and forth and cause the road to become bumpy or the pavement structure to break. This problem can be overcome with several existing methods, including soil improvement, the use of cobweb construction, or using a chicken foot foundation.

Soil improvement methods are generally carried out using selected materials in the foundation layer and stabilization of the foundation. However, this method is still not effective in overcoming the damage to rigid pavement built on soft soil caused by excessive vehicle load and temperature. The application of the cobweb construction system to overcome rigid pavement damage is carried out by utilizing pavement slabs that are stiffened with ribs at the bottom, both longitudinal ribs of the road or diagonal ribs. However, geometrically this method requires special techniques in its work, so it is not suitable to be applied to locations with shallow groundwater levels if the construction is directly placed on the original soil because it has to pump water from the excavation hole and keep the wall from landslides. If the ribs are built first on the work site and then the backfill is carried out, then a compaction method is needed. Meanwhile, using a chicken foot foundation causes excessive road body dropping. The chicken claw foundation is placed on the pile instead of on the soft soil so excessive subsidence occurs due to the consolidation of the soft soil under the pile. However, the decrease that occurred was a uniform decrease so that the road pavement surface still remained flat and comfortable when passed.

Rigid pavement with nailed-slab system is not a type of soil improvement, but is a type of construction used to improve the performance of rigid pavement on soft soil. This pavement system consists of a thin layer of pile covering that serves as a rigid pavement and short piles attached to the bottom. The pile will serve as a nail on the slab so that the slab remains in contact with the base soil. The use of this pavement system will be more durable so that pumping does not occur and differential drop can be reduced [8]. The gap between the pile and the ground around the pile is likely to reduce the friction around the pile which can greatly increase the drop of the rigid pavement slab because the friction that occurs is not thorough along the pile with the gap.

Piles will affect the increase in the reaction modulus on the bed soil. The height of the pile will affect the rigidity of the rigidly attached slab system and reduce the deflection of the slab at the center of load. The nailed slab system will produce uniform drop, increase the bearing strength of the ground, improve the load-bearing capacity and improve the resistance to repeated loads [9]. The nailed slab system was found to be effective in controlling the decrease and increase of the reaction modulus of the bed soil in soft clay soils [10]. [10], [11] propose a system of glued slabs with a thin slab pavement design (12-20 cm) connected to reinforced concrete micropyles with a diameter of 15-20 cm along 1.5-2 meters. The Nailed-slab system will be observed in its behavior on expanding expansive soils. The results show that the upward displacement in the Nailed-slab system is smaller than that of the pileless slab and the soil pavement with piles can reduce the soil heave. [9] found that the installation of piles on the slabs was able to reduce the slab drop and increase the reaction modulus of the base soil. [8] found that all the piles used on the Nailed-slab system produced the same response. The pressure and tensile capacity on the pile are mobilized so that the slab remains in contact with the ground. Piles attached under the slab embedded in the ground increase the rigidity of the slab.

Rigid pavement with Nailed-slab system is a development of the chicken foot foundation method. Rigid pavement with nailed-slab system according to [8] developed by changing the pavement shell of the chicken claw system with short piles. In a road widening project with a foundation pile system, the piles used in the pile have a supporting effect on the pile above it and limit vertical movement on soft soil. The influence of pillars on soft soil deformation only occurs in certain areas and the area will expand as the number of piles increases. The influence boundary of the pile moves towards the axis of the subgrade as the depth increases. The vertical deformation of soft soils reflects peaks that are almost linearly scattered along the depth within the pile's area of influence. The increase in the number of piles causes the linear distribution of deformation that was initially vertical to become slanted and return to the vertical [12]. The use of piles is also used in designing reinforced embankments to maintain stability and subgrade that occurs on soft soils [13] as it allows for rapid highway construction on soft, low-drained soils [14].

Concrete slabs are the most important structural component of rigid pavement. High-performance rigid pavements are often sheathed with a thick base laps and undercoat [15]. The foundation of rigid

pavement generally uses Portland cement concrete (PCC), lean concrete, RCC, or CRC with a very strong load-bearing capacity [16]. According to [17] The use of concrete slabs with rigid pavement can increase resistance to heavy traffic loads, reduce the cost of construction materials, increase service life, increase maintenance intervals and resistance to temperature fluctuations. [18] investigated the impact of Portland cement concrete (PCC) with substandard bending strength on pavement structures under aircraft load conditions. The results show that there is a significant reduction in the cracking performance of the PCC pavement caused by the reduced bending strength. The greater the load of the vehicle, the thicker the concrete slab will be produced and the harder the base soil, the thinner the concrete slab needed must be [19].

Lateral loads and axial loads must be taken into account in designing rigid pavements with a system of Nailed-slabs. Research [6] shows that lateral loads can reduce the carrying capacity of piles, so it is feared that the performance of rigid pavement will decrease as a result of the failure of the pavement structure. The bearing capacity of the pile decreased by 28%, especially the bearing capacity of the friction force of the pile due to the change in gap.

The weakest part of the rigid pavement when subjected to load is the edge of the slab because the wheels of the vehicle that frequently enter and exit can cause cavities in the subbase interface and pavement in long periods of loading. In addition, the bending moment due to temperature will also accelerate damage to the edges of the pavement [20], [21]. In this study, the influence of lateral and axial loads on the behavior of pavement slabs will be examined, including the effect of gaps due to lateral loads on the bearing capacity of pillars and deformation of pavement slabs.

2.0 METHODOLOGY

This research includes quantitative research. Data collection comes from the results of experiments or model-scale experiments in the laboratory. The schematic of the pavement slab with the Nailed-slab system is depicted in Figure 1.

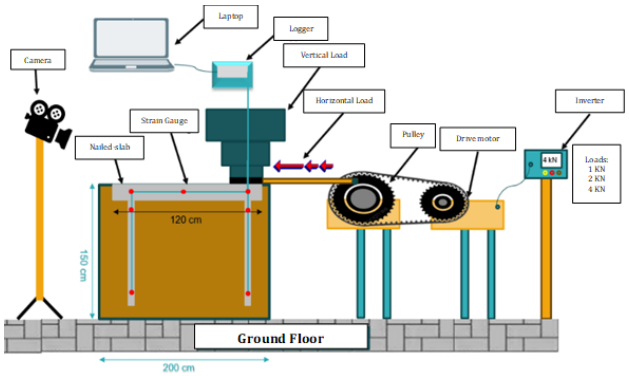

Figure 1 Schematic rigid pavement with nailed-slab system

Based on Figure 1, the distance from the edge of the slab to the wall is 40 cm, while the distance from the pile to the edge of the slab is 1D (10 cm). Therefore, the distance from the pile to the wall of the container box test is 50 cm. This distance meets the minimum requirement for the distance from the pile to the bottom of the container box test, which is 4D, equivalent to 40 cm.

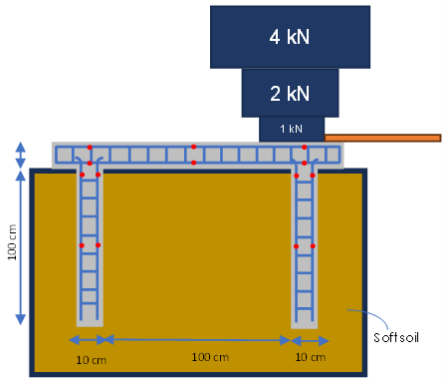

Figure 2 Load and soft soil illustration

The illustration in Figure 2 depicts that the soft soil is placed within the test tank up to a height of 140 cm from the tank floor. The 10 cm-thick plate installed in the tank is not submerged in the soft soil. Before the loading test and numerical test stage on the pavement slab, the steps of this research are:

A. Prototyping

The specifications of the experimental setup, including the body, pile, and slab, are summarized in Tables 1 to 3. The soft soil properties and sampling methods are presented in Table 4, while the types of loads applied during testing are detailed in Table 5. Based on Figure 1, the distance from the edge of the slab to the container wall is 40 cm, and the distance from the pile to the slab edge is 10 cm, meeting the minimum requirement of 4D (40 cm) from the bottom of the container box.

Table 1 *Body planning specifications*

Dimension	=	200 x 200 x 150 cm
Main frame	=	40 x 40 mm (steel L)
Wall	=	- Bottom, side, back of steel slab (t=3 mm) - The front is made of glass material (t=1 cm)
Bottom	=	Water pipes for water outlets

Table 2 Specification of pile and slab

Material	=	Sand and gravel
Cement	=	Portland Cement
Steel slab size plastic	=	Steel reinforcement 8 cm (3 trunk) Mesh width 120 x 120 cm Thick 10 cm
Strain gauge	=	14 pieces - 6 on pavement slabs - 4 each on the pile

Table 3 Specification of nailed-slab

Slab dimensions	=	120 x 120 x 10 cm
Post	=	Depth: 100 cm Diameter: 10 cm
Molding or formwork	=	Multiplex 2 cm Diameter 10 cm (made circular)
Reinforcement	=	Steel 8 mm (diameter)
Waiting process after casting	=	28 days to 100% concrete compressive strength

Table 4 *Soft soil specification*

Origin of the soil	=	Guntur, Demak, Central Java, Indonesia
How to take	=	The soil is due to a depth of 50 cm, cleaned of garbage and organic content mixed with the soil and then put it in a sack to be taken to the laboratory
Tests conducted	=	- Disturbed sampling (ASTM D-1587-94) - Screening analysis (SNI 3423-2008) - Atterberg limit (SNI 1967-2008) - Up to air (SNI 1965-2008) - Specific gravity (SNI 1964-2008) - Direct shear tes (ASTM D-3080-90)

Table 5 *Load type*

Monotonic load	=	Block 20 x 20 cm
Eccentric axial load (gradual)	=	1 kN, 2 kN, 4 kN
Lateral load (from the drive motor)	=	1kN, 2 kN, 4 kN

B. Numerical Test

The numerical test specifications were adjusted to match the laboratory experiments to evaluate differences between the two methods. The loading sequences, including eccentric axial and lateral loads, were applied at 1 kN, 2 kN, and 4 kN, as described in Table 5. This ensures a consistent comparison between experimental and numerical results.

3.0 RESULTS AND DISCUSSION

Demak Soft Soil Testing Result

Soft soil taken from the Guntur area, Demak, Central Java after laboratory tests were carried out to determine its natural properties, the results were obtained in Table 6.

Table 6 Characteristics of soft soil in Demak region, Central Java

No	Characteristics	Value
1.	Specific weight, Gs	2,5
2.	Consistency limits	
	a. Liquid limit, LL	54,5 %
	b. Plastic limit, PL	21,2 %
	c. Shrinkage limit, SL	13,6 %
	d. Plasticity index, PI	33,3 %
3.	Up to air, w	33,1 %
4.	Up fine granules	93,2 %
5.	Sand content	6,8 %
6.	Wet volume weight	17,7 kN/m3
7.	Dry volume weight	13,3 kN/m3
8.	Soil classification	
	a. AASHTO	A-7-5
	b. USCS	CH

The soft soil has a shear strength of 21.4 kPa with an up to Air level of 33.1%. Judging from the size of the soil grains, it is dominated by fine grains of 93.2% and the rest is in the form of fine sand of 6.8% as shown in the grain gradation graph in Figure 3.

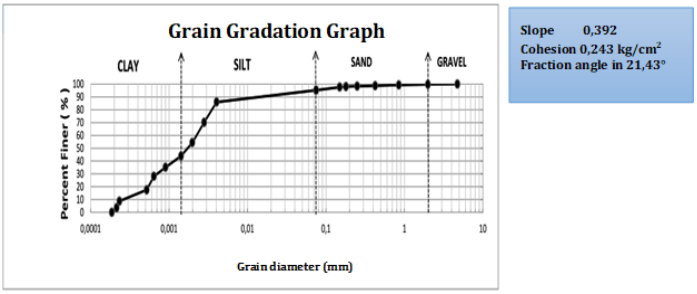

Figure 3 Soft soil grain grading chart

According to the USCS classification, the soft soil from Guntur, Demak that was used as a research sample included the CH classification (high plasticity clay), or equivalent to the A-7-5 classification according to AASHTO, with a PI value of 33.31%. If reviewed against the SL depreciation limit value of 13.62% (>10%), then referring to Almeyer, 1955 this land is not at a critical potential of expansion. So, it can be concluded that the land from Guntur, Demak is a land with a high level of development potential but the potential for expansion is not critical.

Meanwhile, based on the results of the direct shear test in the laboratory, the cohesion value was obtained for a cohesion value of 24.3 kN/m2 and the magnitude of the friction angle in the soil (Ø) 21.43°.

Test Result of Nailed-Slab System

The experimental testing of the Nailed-slab system model was conducted under monotonic loading conditions using a 20 × 20 cm beam. The load was applied incrementally, with each stage representing a twofold increase over the previous load. At the

central loading point, the applied load intensity progressed from P = 0, P = 1 kN, P = 2 kN, to P = 4 kN, which corresponds to 10% of the standard single-wheel load for highways, set at 40 kN. Meanwhile, the edge of the slab was subjected to eccentric axial loads of 1 kN, 2 kN, and 4 kN, respectively. Load-deflection behavior was monitored using strain gauges embedded in the pavement slab. Deflection of the test model as shown in the Table 7.

Table 7 Deflection of the test model

Load (kN)	Longitudinal (mm)		Transverse (mm)	
	Top	Bottom	Top	Bottom
1	0,26	0,25	0,25	0,26
2	0,29	0,27	0,27	0,29
4	0,33	0,30	0,30	0,33

Based on Table 7, the test results indicate that, at a peak load of 4 kN, the maximum deflection observed directly beneath the load was relatively small, measuring approximately 0.33 mm. The deflection pattern observed along the transverse direction, both in the upper and lower reinforcement layers of the Nailed-slab, exhibited a parabolic shape. At the same 4 kN load intensity, the slab edge along the longitudinal direction exhibited a slight downward displacement, which was not significant. Similarly, deflection at the transverse slab edge was negligible. This behavior is consistent with structural expectations, considering the transverse direction represents the shorter dimension of the slab and is supported by underlying piles.

The deflection of the pavement slab at both the upper and lower reinforcement layers indicates that the further the location is from the center of the eccentric axial and lateral loads, the smaller the resulting deflection tends to be. Although the observed deflections are relatively small, they may still contribute to a significant overall deformation of the slab. This is due to the fact that, in addition to receiving eccentric axial loads, the pavement slab is also subjected to lateral loads. The presence of lateral loading causes the supporting piles to undergo lateral deflection, resulting in the formation of a gap around the pile.

This gap formation weakens the bond between the soil and the pile surface, which in turn leads to a reduction in the pile's bearing capacity. Consequently, this reduction in support contributes to further deflection of the pavement slab. Thus, even small initial deflections, if compounded by diminished soil-pile interaction, can result in structurally significant deformations in the slab system.

When evaluated under the standard wheel load of 40 kN (equivalent to a pressure of 566 kN/m²), deflection at both longitudinal edges of the slab remained minor, approximately 0.11 mm. In the transverse direction, the prototype showed edge settlement that is not considered critical in practical applications, as highway construction typically involves segments that are significantly longer than their width. Drawing parallels with rigid pavements employing the Chicken Foot Foundation system which utilizes continuous reinforced slabs the Nailed-slab system is similarly recommended to implement continuous reinforcement. This approach will mitigate significant edge deflection in field implementations, thereby enhancing structural performance and serviceability.

Numerical Analysis of Nailed-Slab

The numerical analysis of the nail plate was adjusted to the laboratory test so that the results were not significantly different. The loading (lateral and axial) on the nail plate was given sequentially at 1 kN, 2 kN, and 4 kN with a loading duration of 20 seconds each. The results showed that the eccentric axial and lateral loads resulted in the collapse of the pile. The input data in the 3D FEM model are as shown in Table 8.

Table 8 Input Parameters for 3D FEM Modeling

Parameter	Soil	Pile	Slab
Material model	Mohr-coulomb	Elastic	Elastic
Material behavior	Undrained	Non-porous	Non-porous
Saturated unit weight	17,7 kN/m³	24 kN/m³	24 kN/m³
Dry unit weight	13,3 kN/m³	-	-
Young's modulus	18.000 kPA	-	-
Poisson's ratio	0,30	-	-
Undrained cohesion	18,00 kPA	-	-
Internal friction angle	21,43°	-	-
Dilation angle	0,00°		
Initial void ratio	0,872	-	-
Interface strength ratio	0,90	0,90	0,90

Based on the Table 8, the input data in the 3D FEM test was adjusted to the data in the laboratory test so that the results in the 3D FEM test are expected to be close to the results of the laboratory test. The results of the 3D FEM model testing are depicted in Figures 4 and Figure 5.

Based on Figure 4 (a) and (b), the maximum deflection pattern in the longitudinal direction of the Nailed-slab, particularly at the top reinforcement layer as observed in the laboratory model test, indicates that deflection tends to decrease as the distance from the center of the eccentric axial load increases. Nevertheless, the overall deflection observed in the pavement slab is considered significant, due to the initial formation of a gap around the pile caused by lateral loading. This gap contributes to a reduction in the pile's bearing capacity, which subsequently leads to additional slab deflection. [22] in his research on the analysis of piles due to lateral loads, said that the gap that occurs between the pile and the surrounding soil greatly influences the loading that occurs, the greater the lateral load on the pile, the greater the gap that occurs between the pile and the soil.

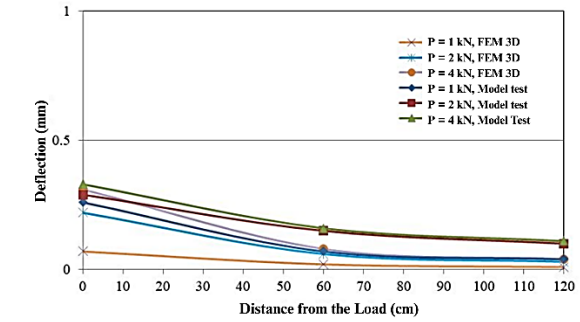

(a) Top Reinforcement

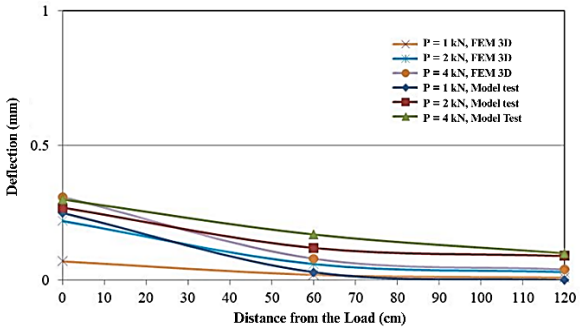

(b) Bottom Reinforcement

Figure 4 Comparison of longitudinal deflection patterns

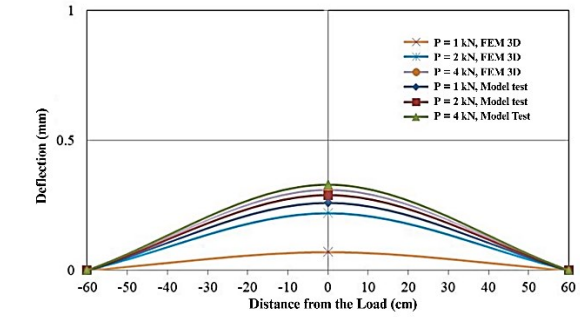

(a) Top Reinforcement

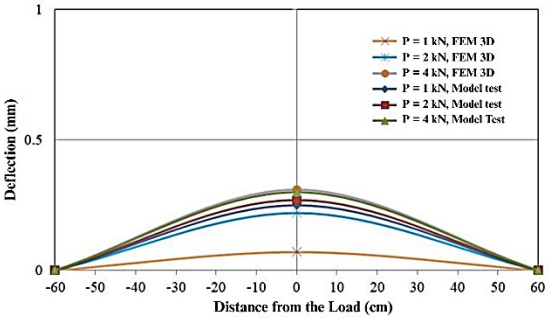

(b) Bottom Reinforcement

Figure 5 Comparison of transverse deflection patterns

Similarly, the finite element method (FEM) analysis also confirms the same trend in the longitudinal direction of the Nailed-slab reinforcement. The deflection of the pavement slab decreases with increasing distance from the point of eccentric axial loading. However, the overall slab deformation remains significant due to the emergence of gaps around the pile. These gaps are attributed to the combined effects of varying eccentric axial loads and lateral loads, both of which contribute to the reduction of the pile's bearing resistance. This loss of support is directly associated with increased deflection of the pavement slab. From the 3D FEM simulation results, it was found that the maximum deflection of the pavement slab reached approximately 31%, indicating a substantial deformation under the applied loading conditions.

The deflection pattern in the transverse direction at the bottom reinforcement layer of the pavement slab, as observed in both the laboratory model and the 3D FEM simulation, exhibits a parabolic shape. In this direction, the edge regions of the slab show insignificant deflection, which can be rationalized by the fact that the transverse side represents the shortest span of the slab, and is directly supported by two piles. These piles serve to resist the combined effects of eccentric axial and lateral loading, thereby limiting transverse deflection.

From the 3D FEM analysis, minimal deflection is also observed at both transverse edges of the slab, that is, away from the center of lateral loading. The numerical simulation was conducted using identical parameters to those used in the laboratory testing, including the container box test dimensions, prototype model geometry, soil properties, slab material, and pile characteristics.

The results confirm that the deflection pattern in the longitudinal direction closely resembles the one recorded in the physical test. Specifically, deflection tends to decrease with increasing distance from the center of the eccentric axial and lateral load. A noticeable deflection occurs near the longitudinal edges, which is attributed to the influence of lateral loading applied near the slab center. [23] conducted a laboratory-scale study on a single pile under fixed conditions subjected to lateral loading. The research aimed to investigate the effect of lateral load on various sections of the pile in relation to its deflection. The results revealed that, under the same lateral load, the greatest deflection occurred at the top end of the pile.

Similarly, in the transverse direction, the deflection pattern shows that as the distance increases from the center of the eccentric axial and lateral load toward the slab edge, the deflection values decrease gradually, approaching zero. The minimal edge deflection in the transverse direction occurs because the applied loads are first resisted by the two supporting piles, thus significantly reducing the transferred stress and deformation to the outer portions of the slab. As [24] the greatest deflection occurs in the center of the plate with the greatest load, while at two points at the ends of the plate the deflection is smaller. Reducing the load to 0 kN causes the plate to return to its original state without receiving a load (0 kN).

So based on the results of model and simulation tests (FEM 3D), it is known that the highest deflection occurs just under the load and decreases as the distance increases. In addition, the amount of deflection that occurs is influenced by the magnitude of the load. The greater the load given, the greater the deflection that occurs. The results of the simulation (FEM 3D) there is a slight difference in the results that may be caused by assumptions in the simulation. However, the results of the 3D FEM simulation are able to represent the behavior of materials well. The comparison of the resulting deflection results from the two-test method is described in Table 9.

Table 9 Comparison of highest deflection results

Deflection	Maximum Deflection Value (in mm)	
	Test Model	Simulation (FEM 3D)
Slab deflection	0,33	0,31
Pile deflection	0,24	0,22

Based on Table 9. It can be explained that in both slab deflection and pile deflection there is a difference of 0.02 mm between the model test results and the simulation (FEM 3D). The results from the 3D FEM simulation indicate minor discrepancies when compared to the experimental data, which are likely due to assumptions made during the simulation process. Nevertheless, the FEM 3D simulation is considered effective in accurately representing the material behavior and structural response of the system. This shows that the simulation results (FEM 3D) are close to the real test results with a small difference in the resulting deflection values, so that the simulation (FEM 3D) can be used as a valid tool to predict structural deformations in slabs and posts. The small deviation also indicates that the method is representative enough to replicate real conditions so that it can reduce the need for expensive and time-consuming physical testing.

4.0 CONCLUSION

The Nailed-slab tested in the laboratory has a size of 1.2 x 1.2 m with a slab thickness of 10 cm. On the Nailed-slab there are four micro (short) piles with a diameter of 10 cm, a length of 100 cm which are installed at a distance of 100 cm. Based on the test results, the Nailed-slab system can be applied in road pavement. The wider the form of application, the more piles are used. Some of the advantages that can be obtained when using this nailed-slab system include that the construction is easier because it uses short micro piles and does not require heavy equipment to work on it so it does not take a long time and construction costs tend to be lower. This nailed-slab system also does not require a temporary pavement as a working mat for heavy vehicles to pass, so it is very promising to be applied in the field.

Acknowledgement

Thanks to all parties involved, especially the engineering laboratory team of Sultan Agung Islamic University.

Conflicts of Interest

The authors declare that there is no conflict of interest regarding the publication of this paper.

References

[1] Fang, M., R. Zhou, W. Ke, B. Tian, Y. Zhang, and J. Liu. 2022. Precast System and Assembly Connection of Cement Concrete Slabs for Road Pavement: A Review. *Journal of Traffic and Transportation Engineering*. https://doi.org/10.1016/j.jtte.2021.10.003.

[2] Singh, R. R., M. Hasnat, M. E. Kutay, S. W. Haider, J. Bryce, and B. Cetin. 2024. Condition Indices for Rigid Pavements: A Comparative Analysis of State DOTs Using Michigan PMS Data." *Journal of Road Engineering*. 4(3): 348–360. https://doi.org/10.1016/j.jreng.2024.05.003.

[3] Mohammadinia, A., M. M. Disfani, G. A. Narsilio, and L. Aye. 2018. Mechanical Behaviour and Load Bearing Mechanism of High Porosity Permeable Pavements Utilizing Recycled Tire Aggregates. *Construction and Building Materials*. 168: 794–804. https://doi.org/10.1016/j.conbuildmat.2018.02.179.

[4] Qin, Y., and J. E. Hiller. 2011. Modeling Temperature Distribution in Rigid Pavement Slabs: Impact of Air Temperature." *Construction and Building Materials*. 25(9): 3753–3761. https://doi.org/10.1016/j.conbuildmat.2011.04.015.

[5] Tang, C., J. Liu, Z. Lu, Y. Zhao, J. Zhang, and Y. Feng. 2024. Dynamic Thermo-Mechanical Responses of Road-Soft Ground System under Vehicle Load and Daily Temperature Variation. *Journal of Rock Mechanics and Geotechnical Engineering*. 16(5): 1722–1731. https://doi.org/10.1016/j.jrmge.2023.07.023.

[6] Situmorang, A., and A. Rochim. 2019. The Changes of Friction Capacity of the Pile to Support Slab Pavement Due to Lateral Loads. *International Journal of Civil Engineering and Technology*. 10(11): 66–71.

[7] Beskou, N. D., and E. V. Muho. 2023. Review on Dynamic Response of Road Pavements to Moving Vehicle Loads; Part 1: Rigid Pavements. *Soil Dynamics and Earthquake Engineering*. https://doi.org/10.1016/j.soildyn.2023.108249.

[8] Puri, A., H. C. Hardiyatmo, B. Suhendro, and A. Rifa'i. 2019. Validating the Curve of Displacement Factor Due to Full Scale of One Pile Row Nailed-Slab Pavement System. *International Journal of GEOMATE*. 17(59): 181–188. https://doi.org/10.21660/2019.59.65815.

[9] Waruwu, A., H. C. Hardiyatmo, and A. Rifa'i. 2017. Deflection Behavior of the Nailed Slab System-Supported Embankment on Peat Soil. *Journal of Applied Engineering Science*. 15(4): 556–563. https://doi.org/10.5937/jaes15-15113.

[10] Diana, W., H. C. Hardiyatmo, and B. Suhendro. 2017. Effect of Pile Connections on the Performance of the Nailed Slab System on Expansive Soil. *International Journal of GEOMATE*. 12(32): 134–141. https://doi.org/10.21660/2017.32.42773.

[11] Diana, W., H. C. Hardiyatmo, and B. Suhendro. 2016. Small-Scale Experimental Investigation on the Behaviour of

Nailed Slab System in Expansive Soil. In *AIP Conference Proceedings*. https://doi.org/10.1063/1.4958493.
[12] Chen, T., and G. Zhang. 2024. Centrifuge Modeling of Pile-Supported Embankment on Soft Soil Base for Highway Widening." *Soils and Foundations*. 64(1). https://doi.org/10.1016/j.sandf.2023.101422.
[13] Zhang, D., G. Yang, X. Wang, Z. Wang, and H. Wang. 2022. Analysis of Load Transfer and the Law of Deformation within a Pile-Supported Reinforced Embankment. *Applied Sciences*. 12(23). https://doi.org/10.3390/app122312404.
[14] Onur, M. İ., and E. Balaban. 2018. A Numerical Model on Geosynthetic Reinforced Pile Supported Embankments. *Anadolu University Journal of Science and Technology A*. (Applied Sciences and Engineering). https://doi.org/10.18038/aubtda.376144.
[15] Gohil, R. R., V. Samu, and J. Kumar. 2024. Non-Destructive Evaluation of Rigid Pavements Using Surface Wave Tests. *Construction and Building Materials*. 442. https://doi.org/10.1016/j.conbuildmat.2024.137651.
[16] Liu, Z., S. Yu, Y. Huang, L. Liu, and Y. Pan. 2024. A Systematic Review of Rigid-Flexible Composite Pavement. *Journal of Road Engineering*. https://doi.org/10.1016/j.jreng.2024.02.001.
[17] Fattouh, M. S., B. A. Tayeh, I. S. Agwa, and E. K. Elsayed. 2023. Improvement in the Flexural Behaviour of Road Pavement Slab Concrete Containing Steel Fibre and Silica Fume. *Case Studies in Construction Materials*. 18. https://doi.org/10.1016/j.cscm.2022.e01720.
[18] Robinson, W. J. 2024. Evaluating the Influence of Flexural Strength on Rigid Pavement Performance under Simulated Aircraft Traffic. *Construction and Building Materials*. 449. https://doi.org/10.1016/j.conbuildmat.2024.138486.
[19] Costarico, M. T., M. M. Iqbal, and J. Arliansyah. 2019. Effects of the Design Parameters against Slab on Grade Volume Using Corps of Engineering Design Method. In *Journal of Physics: Conference Series*. https://doi.org/10.1088/1742-6596/1198/8/082001.
[20] Puri, A., B. Suhendro, and A. Rifa'i. 2017. Effects of Vertical Wall Barrier on the Rigid Pavement Deflection of Full Scale 1-Pile Row Nailed-Slab System on Soft Subgrade. *International Journal of GEOMATE*. 12(32): 25–29. https://doi.org/10.21660/2017.32.6577.
[21] Puri, A., and M. Toyeb. 2020. Numerical Analysis of Nailed-Slab Pavement System by Considering a Void under the End of Slab. *International Journal of GEOMATE*. 18(66): 50–55. https://doi.org/10.21660/2020.66.9306.
[22] Chandrasekaran, S. S., A. Boominathan, and G. R. Dodagoudar. 2008. Behaviour of 2 × 2 Pile Group under Static and Cyclic Lateral Loading. *Indian Geotechnical Journal*. 38(4): 413–432.
[23] Khari, M., K. A. Kassim, and A. Adnan. 2014. Development of p-y Curves of Laterally Loaded Piles in Cohesionless Soil. *The Scientific World Journal*. 2014. https://doi.org/10.1155/2014/917174.
[24] Puri, A., H. C. Hardiyatmo, B. Suhendro, and A. Rifa'i. 2014. Behavior of Nailed-Slab System on Soft Clay Due to Repetitive Loadings by Conducting Full Scale Test. *International Journal of Civil & Environmental Engineering*. 14(6): 24–30.